Journal of Organometallic Chemistry, 478 (1994) 213–221

Electronic structure of exohedral interactions between C_{60} and transition metals

Dennis L. Lichtenberger, Laura L. Wright *, Nadine E. Gruhn and Margaret E. Rempe

Department of Chemistry, University of Arizona, Tucson, AZ 85721 (USA)

(Received December 6, 1993; in revised form February 22, 1994)

Abstract

The electron distribution and orbital interactions of C_{60} with metals coordinated at different sites on the outside of the fullerene are evaluated. These sites include the position of a metal atom directly above a carbon atom (η^1 site), the metal atom centered above two carbons of a pentagon or above two carbons between two pentagons (both η^2 sites), the metal atom centered above a pentagon (η^5 site), and the metal atom centered above a hexagon (η^6 site). The frontier orbitals of C_{60} are illustrated first with three-dimensional orbital contour plots. A palladium atom is then used to probe the bonding at the different sites on the C_{60} surface. The results with Pd^0 are compared to our earlier study with the harder Ag^+ ion in order to examine the effects of metal electron richness and size. In addition, these results are compared with the bonding to more traditional ligands that represent the hapticity of these sites, such as methyl (η^1), ethylene (η^2), cyclopentadienyl (η^5), and benzene (η^6). The strength of the metal–C_{60} interaction and the amount of charge delocalized from the metal to C_{60} is sensitive to the site of coordination, the electron richness of the metal, and distortions in the geometry of C_{60}. As discussed in our previous work, the frontier orbitals of C_{60} are well-suited for synergistic bonding of a metal atom to a carbon–carbon pair in an alkene-like fashion, in which the HOMO of C_{60} donates carbon–carbon π bonding electron density to the metal, and the LUMO of C_{60} accepts electron density from the metal into a carbon–carbon π^* antibonding orbital. Although the HOMO and LUMO of C_{60} describe the basic interaction, many frontier orbitals are involved. The site above the C–C bond between two pentagons is favored over the site above the C–C bond within a pentagon, and the interaction above the other sites is indicated to be net repulsive by these calculations. The differentiation between these sites increases with the electron richness of the metal center. The bonding of the metal to C_{60} is generally weaker than to the small ligands, except for very electron rich metal centers where the bonding to the η^2 site between pentagons apparently becomes stronger than the bonding to ethylene.

Key words: Silver; Palladium; Fullerenes; Electronic structure; Molecular orbital; Transition metals

1. Introduction

While early experimental studies on C_{60} concentrated on identifying and isolating this material [1], more recent research interests involving fullerenes have become greatly diversified [2]. One growing interest has been in the chemistry of C_{60} with metals, with potential applications based on special properties that arise from the unique spherical structure of C_{60} and the framework of partially delocalized carbon π orbitals [3]. Every carbon atom in C_{60} is chemically equivalent, however, the structure of C_{60} offers many different possible bonding sites and modes of interaction with metals, as shown below. Bonding sites are labelled with numbers corresponding to hapticity. The site directly above a carbon atom is η^1 and is labeled site **1**. The sites centered above the pentagons (η^5) and hexagons (η^6) are labelled **5** and **6** respectively. There are two different types of carbon–carbon bonds in C_{60} available for η^2 coordination to a metal center, and these are labelled **2′** and **2″**. Other less-symmetrical bonding modes, such as η^4 or η^3, are also available.

In one η^2 type of site each carbon atom of the pair is a member of a different pentagon, and the bond joins the two pentagons. These bonds will be referred to as the bonds between pentagons and they correspond to the **2″** positions for coordination of a metal

Correspondence to Prof. D.L. Lichtenberger.
* Permanent address: Department of Chemistry, Furman University, Greenville, SC 29613, USA.

0022-328X/94/$7.00
SSDI 0022-328X(94)24629-W

© 1994 – Elsevier Science S.A. All rights reserved

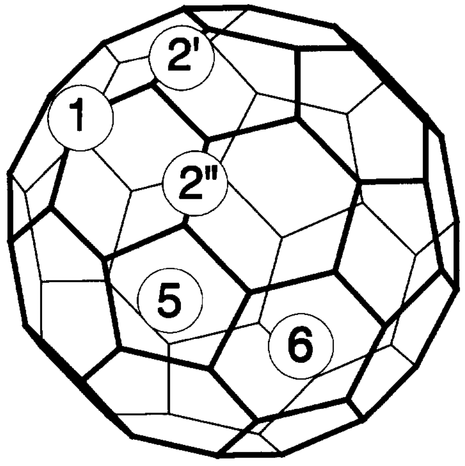

atom. These bonds are often referred to as the fusion between two six-membered rings. However, these fusions between six-membered rings are different from those that occur in graphite and polyaromatic hydrocarbons. More important than the fusion of six-membered rings is recognition that these bonds connect two different pentagons. It is the occurrence of the pentagons that leads to the curvature of the structure and the special properties of C_{60}. The connection of pentagons also occurs in the structure of C_{70}, with similar chemical effects [4]. The structure of C_{70} has other 6:6 ring fusions that do not connect pentagons, and these sites do not show the same reactivity. Therefore we prefer calling the site between pentagons the **2″** position rather than the 6:6 ring fusion. The other type of carbon–carbon bond in C_{60} has both carbon atoms within the same pentagon (a 6:5 ring fusion). These will be referred to as the bonds within pentagons or the **2′** positions.

C_{60} has been shown to form several interesting organometallic complexes, and definite bonding trends have been identified [4–15]. In organometallic complexes the picture that emerges is that C_{60} prefers to coordinate as an electron deficient η^2-alkene-like fragment with the metal at the **2″** position. The amount of charge withdrawn from the metal by C_{60} is intermediate between that withdrawn by ethylene and tetracyanoethylene (TCNE).

Many electronic structure calculations on C_{60} have been carried out at different levels of approximation. Most of these have dealt with bond lengths, orbital energies and other properties of C_{60} alone [16]. Few have explored the structure and bonding characteristics of the organometallic derivatives [17]. A recent paper by Rogers and Marynick examines the possibilities of binding C_{60} in an η^6 fashion [18]. The bonding of C_{60} and benzene to the $Cr(CO)_3$ fragment were compared. In this study C_{60} was shown to be bound much more weakly than benzene to the metal. Koga and Morokuma have reported a molecular orbital calculation on the model compound $(\eta^2\text{-}C_{60})Pt(PH_3)_2$ in comparison to $(\eta^2\text{-}C_2H_4)Pt(PH_3)_2$ [19]. They found that $Pt(PH_3)_2$ donates electron density much more strongly to C_{60} than to ethylene and forms a stronger bond. Other bonding modes have not been explored and compared.

The traditional scheme to describe the bonding of an alkene or other unsaturated organic fragment to a metal utilizes donation from the occupied π orbitals of the fragment to empty metal orbitals with simultaneous back-donation from occupied metal d orbitals into the empty π^* orbitals on the fragment [20]. Key questions are whether C_{60} has orbitals of appropriate symmetry, energy, and overlap with a metal at different sites for bonding in this manner. If the orbitals are available, what is the relative extent of electron donation and acceptance? In our previous paper the orbital nodal characteristics of C_{60} were examined in terms of a fragment analysis and the different bonding sites were probed using a "hard" Ag^+ ion [17]. Here we report the effects of probing with a "soft" metal center at the different sites on the C_{60} molecule, and compare the bonding to other simple organic ligands. For purposes of comparison, we choose Pd^0 as the probe. This choice is not entirely theoretical in nature. Palladium has recently been reported to form the first organometallic polymer with C_{60} [21]. The polymer has the formulation $C_{60}Pd_n$ and it is proposed that each palladium atom is bound to the π electron surface of two C_{60} molecules in a dumbbell fashion.

2. Methods

The purpose of this investigation is to further examine the orbital overlap interactions between C_{60} and metals in order to better understand the reactivity trends. Calculations are carried out using the Fenske-Hall method [22] in exactly the same manner as our previous publication [17]. New programs which we have developed for the three-dimensional representation of molecular orbitals which were not available at the time of our previous study have been employed here [23]. The Fenske-Hall method is an approximate, non-empirical molecular orbital method that has been used extensively for investigation of the electronic structure and bonding of inorganic and organometallic molecules. The method contains the essential elements of orbital overlaps, charge distributions, and energies that are suitable for the purposes of this investigation. An advantage of the method for this study is that it allows efficient evaluation and comparison of the individual electronic structure interactions of several different conformations. The method has been successful in reproducing and predicting trends in electronic structure properties between related molecules, particularly as shown by high resolution valence photoelectron spectroscopy [24]. The disadvantage of this approach is that the approximations of the method have not been optimized to provide reliable total energies for direct studies of potential surfaces related to reaction coordinates or geometry distortions. For this reason, the calculations are generally carried out for geometries that are determined either experimentally or by other theoretical means.

The truncated icosohedron structure of C_{60} is completely determined by two bond lengths, the C–C length within the pentagons, and the C–C length between the pentagons. The bond lengths for C_{60} used in these calculations are from the geometry optimized by Scuseria (1.372 Å between pentagons, 1.453 Å within pentagons) [25]. These are within 0.02 Å of the bond distances determined experimentally by solid-state X-ray diffraction [26] and gas phase electron diffraction [27]. In order not to bias the origin of the changes in bonding and charge distributions within the C_{60} molecule when it is coordinated to metals, these bond lengths are initially left constant in all calculations. Distortions in these geometries will be considered subsequent to the changes in electronic structure, as described in the results and discussion section. The internal bond distances and bond angles of the small ligand counterparts of the various bonding sites were also idealized for purposes of this comparison. Ethylene, benzene and cyclopentadienyl were all taken as planar. For the calculations of a metal coordinated to different sites of C_{60} and to small ligand counterparts, the distance between the bound carbon atoms and the metal is based on the structure of $(\eta^2\text{-}C_{60})Pd(PPh_3)_2$ [15]. In all cases the metal is positioned 2.10 Å from the nearest carbon atoms, and the z-axis of the metal is directed at the center of the bonding site. When the metal is coordinated to the η^2 positions, the carbon atoms are in the xz plane.

3. Results and discussion

In our previous publication of studies on the interaction of C_{60} with metals [17], the nodal properties of the frontier orbitals of C_{60} were discussed and illustrated. The frontier orbitals are most easily understood in terms of a fragment analysis. In one view, the molecule is composed of the 12 pentagons and the frontier orbitals of C_{60} are composed of linear combinations of the familiar orbitals of the cyclopentyl group. It was found that the e_1'' combination of the pentagon carbon p_π orbitals (a single node perpendicular to the C_5 plane) is the primary contribution to the frontier

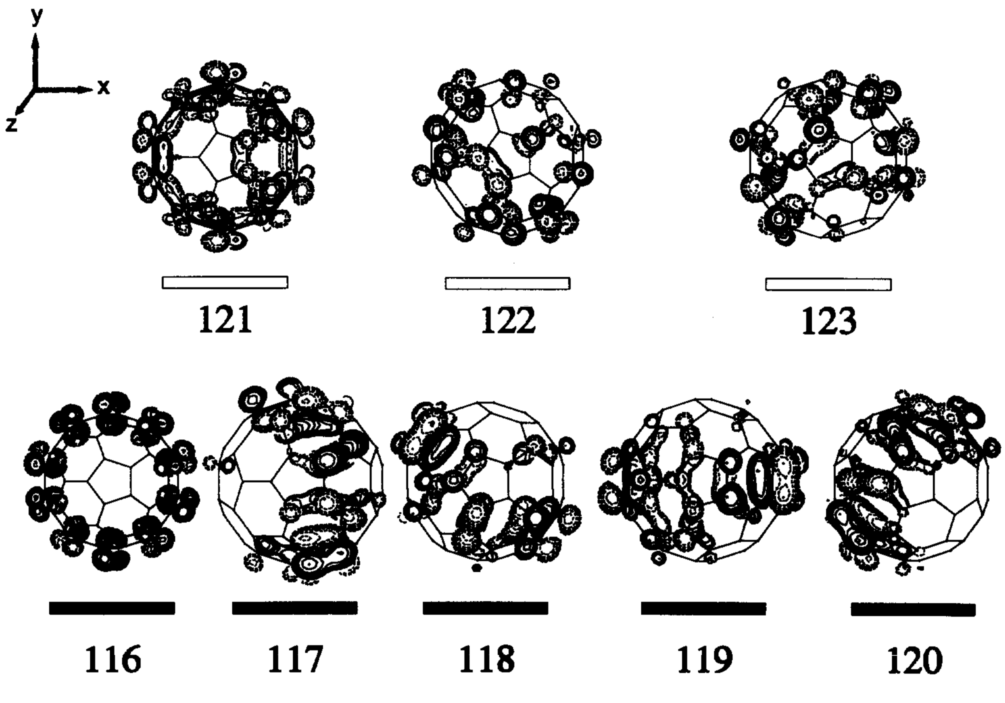

Fig. 1. Orbital surface plots (value = ± 0.03) of the five degenerate orbitals of the h_u symmetry HOMO (116–120) and the three degenerate orbitals of the t_{1u} symmetry LUMO (121–123) of C_{60}.

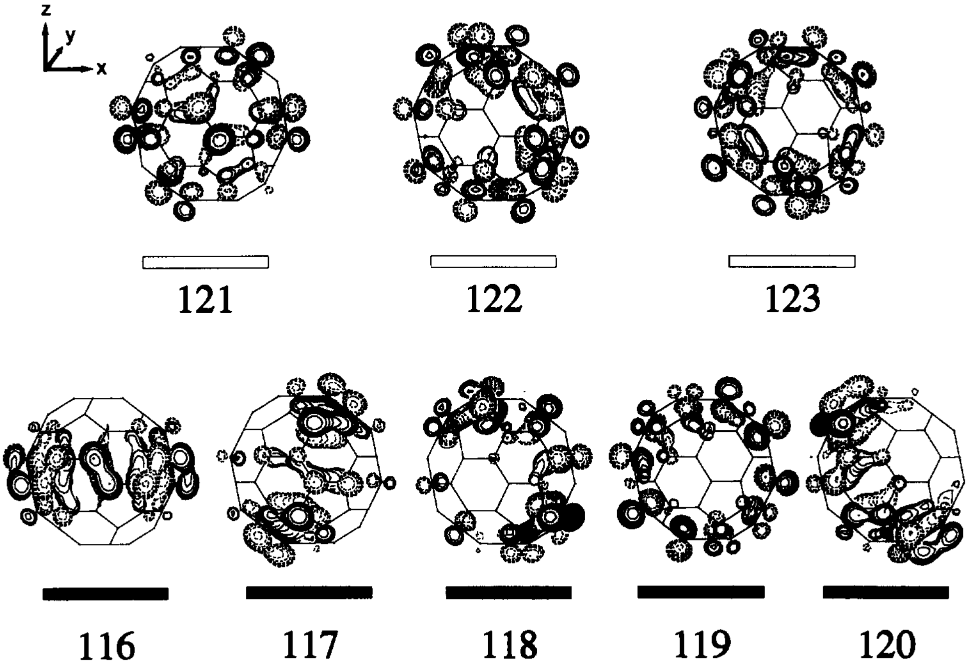

Fig. 2. Orbital surface plots of the orbitals in Fig. 1 rotated 90°.

orbitals. In another view, C_{60} is composed of the 30 C_2 units that represent the 2″ positions between the pentagons. In this case the frontier orbitals are simply described in terms of linear combinations of the π and π^* orbitals of an alkene. It was found that the C_2 units are a better (more complete) description of the frontier orbitals of C_{60} in terms of the total character of the orbitals.

Even with these descriptions, it is difficult to obtain a total appreciation for the nodal characteristics of these orbitals without a visual representation. We find the three-dimensional renderings of these orbitals to be enlightening, not only conceptually, but also in relation to experimental properties of C_{60}. One example of the value of visualization is the localized molecular orbitals of C_{60}, which emphasizes the single bond character between the carbons in the pentagons (2′ positions) and the double bond character between the carbons between pentagons (2″ positions) [28]. The visualization of the canonical orbitals has been most revealing in relation to the STM images of C_{60} on gold, where the contrasts in the STM images are directly related to the spatial distributions of the LUMOs of C_{60} [29]. Figure 1 shows a three-dimensional representation of the HOMO (h_u molecular orbitals 116–120 of the 240 valence molecular orbitals of C_{60}) and LUMO (t_{1u}, orbitals 121–123) of C_{60} viewed down the center of a pentagon. Figure 2 shows the same orbitals as Fig. 1 viewed at a 90° rotation, such that the central pentagon in Fig. 1 is at the top in Fig. 2. Because each set

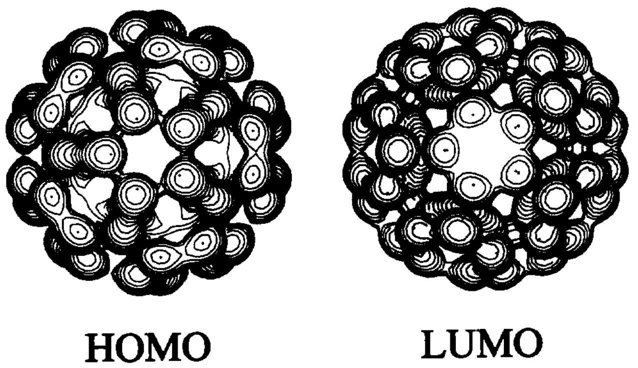

Fig. 3. Surface density plots of a fully occupied h_u HOMO (value = 0.002 $e^-/(au)^{-3}$) and a fully occupied t_{1u} LUMO (value = 0.0012 $e^{-1}\backslash(au)^{-3}$).

of orbitals is degenerate, any rotation (linear combination) among the orbitals in a set gives an equivalent total representation. Interesting bonding and antibonding patterns can be identified in these representations. In the HOMO, electron density appears to be distributed in "belts" around the sphere, while the electron density is distributed more evenly throughout the sphere in the LUMO. The C–C p_π bonding character of the HOMO at the 2″ position is shown most clearly in orbital 116 in Fig. 2. In terms of a fragment orbital basis decomposition analysis, the HOMO is 77% comprised of the C–C p_π bond at these positions [17]. Similarly, the C–C p_π antibonding character at the 2″ position is observed in the LUMO orbital 121, Fig. 2. The fragment basis analysis shows that the LUMO is 92% comprised of the C–C p_π antibond [17]. Another familiar pattern is the e_1'' orbital of a five-carbon ring which is clearly observed in orbitals 119, 122, and 123 of Fig. 1. In terms of a fragment basis of the pentagons, the HOMO and LUMO are 63% and 72%, respectively, comprised of the e_1'' symmetry p_π orbitals of the pentagons [17].

It is also instructive to look at the total electron density provided by two electrons in each of the five orbitals of the h_u symmetry HOMO. The sum of these five orbital densities is shown in the surface plot of Fig. 3. It is clearly seen that the h_u orbitals are net π bonding between the pentagon rings at the 2″ positions, and net π antibonding between the carbons within the pentagons at the 2′ positions. Similarly, the electron density plot assuming two electrons in each of the three orbitals of the t_{1u} LUMO is also shown in Fig. 3. Here the reverse is seen. The t_{1u} orbitals are not π antibonding at the 2″ positions, and net bonding between the carbons within the pentagons. Thus the HOMO and LUMO orbitals are set up very well for donation and acceptance in interactions with metals at the 2″ positions. As will be seen, these HOMO and LUMO orbitals provide a good qualitative understanding of the interactions of C_{60} with transition metals, but several other frontier orbitals are also important for understanding the total interaction. Other orbitals that are close in energy to the HOMO and LUMO were discussed in our earlier work [17].

For the next step in examination of the orbital factors that contribute to the coordination of a transition metal atom to the surface of C_{60}, we have carried out calculations where Ag^+ [17] or Pd^0 are coordinated at the different sites described in the introduction. Both Ag^+ and Pd^0 have filled d-orbital shells available for electron donation to empty orbitals of C_{60}, and they have empty 5s and 5p orbitals available for accepting electron density from filled orbitals of the C_{60}. Thus both have the necessary symmetry orbitals and occupations to probe the electronic interactions at the various bonding sites. However, Ag^+ and Pd^0 differ in the relative "hardness" that they exhibit in bonding to ligands. The Ag^+ ion is a relatively "hard" probe in the sense that electron donation from the d orbitals to C_{60} is expected to be relatively small. For instance, other calculations have shown that the interaction of Ag with ethylene is weak [30]. In comparison, Pd^0 is a relatively "soft" probe, and is much more willing to give up electron density. We also include calculations of Ag^+ and Pd^0 with methyl, ethylene, cyclopentadienyl, and benzene for the purpose of comparison.

The pertinent results of the calculations on the interaction of the Ag^+ ion with the different sites on C_{60} and the corresponding smaller ligands are summarized in Table 1. As mentioned before, in addition to the HOMO and LUMO of C_{60} a large number of the other frontier orbitals of C_{60} are involved in electron donation and acceptance with the metal center. By focusing on the electron distributions in the different symmetry metal orbitals instead of the different C_{60} orbitals, it is easy to evaluate the total electron delocalization between the metal and C_{60}. The most important trends are seen by looking at the metal 5s interaction, which is accepting electron density from C_{60} in a σ symmetry interaction, and the metal $4d_{xz}$ interaction, which is capable of donating electron density to the C_{60} in a π symmetry interaction. The metal 5p orbitals make negligible contributions to the frontier orbitals in these calculations. Orbital and overlap populations for 5s and $4d_{xz}$ orbitals are tabulated. The d orbitals that are not the correct symmetry for donation into the t_{1u} orbital remain doubly occupied and are

TABLE 1. Mulliken orbital population analysis for silver orbitals coordinated to various small ligands and C_{60} sites

	Methyl	Ethylene	Cp	Bz	C_{60} Site 1	C_{60} Site 2′	C_{60} Site 2″	C_{60} Site 5	C_{60} Site 6
Ag^+ $4d_{xz}$ population	1.996	1.842	1.808	1.901	1.996	1.918	1.910	1.909	1.908
Ag^+ 5s population	0.270	0.281	0.102	0.056	0.299	0.289	0.325	0.121	0.090
Ag^+ total 4d overlap population	+0.075	+0.038	−0.008	−0.115	−0.047	−0.048	−0.023	−0.170	−0.238
Ag^+ $4d_{xz}$ overlap population	−0.015	+0.095	+0.001	−0.081	−0.032	+0.018	+0.036	−0.064	−0.085
Ag^+ 5s overlap population	+0.173	+0.211	+0.034	−0.021	+0.143	+0.132	+0.157	+0.033	−0.003

dominated by destabilizing filled-filled interactions with the C_{60}. This is seen in the Ag^+ total 4d overlap populations with C_{60}. Partly for this reason, the interaction of Ag^+ with each site on C_{60} is destabilized relative to the interaction with the smaller ligands.

Donation from the Ag^+ d orbitals to C_{60} is most effective for the **2″**, **5**, and **6** positions. For the metal in the **2″** position, the total donation is about 0.09 e^-, but only about 0.015 of those electrons reside in the appropriate C_{60} LUMO t_{1u} orbital. This emphasizes the point that a large number of the frontier orbitals are mixed by the interaction with the metal center. Donation from C_{60} to the 5s orbital of Ag^+ is clearly most effective for the **2″** position. The overlap populations between the Ag^+ orbitals and C_{60} lead to similar conclusions. The **2″** position significantly favors both σ donation and π acceptance by C_{60}. This is the site occupied by the metal in all complexes that have been structurally characterized to this time. An important point to note from the tabulated data is that in each case the bonding at a given C_{60} site is weaker than with the corresponding small ligand. Rogers and Marynick obtained a similar result in the comparison of the bonding of C_{60} and benzene to a metal [18]. Thus even though the frontier orbitals are energetically favorable for delocalization of electron density with the metal center, the spatial distribution of the frontier orbitals of C_{60} does not favor overlap comparable to the small ligands. For instance, even though C_{60} delocalizes more electron density to the 5s orbital of a metal in the **2″** position than does ethylene, the overlap population of the 5s orbital with C_{60} is less than with ethylene.

Table 2 summarizes the results of similar calculations with the "softer" Pd^0 probe. As expected, donation from the $4d_{xz}$ orbital is greater and acceptance by the 5s orbital smaller for Pd^0 compared to Ag^+. As observed in the silver case, the palladium-small ligand interactions are stronger than the interactions with the corresponding C_{60} sites. The **2″** position is once again the favored C_{60} sites. The metal d_{xz} orbital donates about 0.29 e^- to the C_{60}, and about 0.09 of this charge is in the appropriate orbital of the C_{60} LUMO t_{1u}. The repulsions between C_{60} and the filled metal orbitals are substantial, so that the overall 4d and 5s overlap populations are positive only for the **2″** position on C_{60} in which the 5s and $4d_{xz}$ interactions are most favorable. The relatively high 5s population at the **2″** site compared to other C_{60} sites shows that the donation to the metal is most efficient to this site, but again the overlap population of the 5s with C_{60} is relatively low.

It is interesting to consider the mobility of the metal on the surface of C_{60} between different **2″** sites. This requires that the metal traverse orientations either at or close to the other sites. For example, one path between **2″** sites proceeds across site **1** (η^1) to site **2′** and on to the next site **1** and the next site **2″** as shown in path **A** below. Another possible route is across site

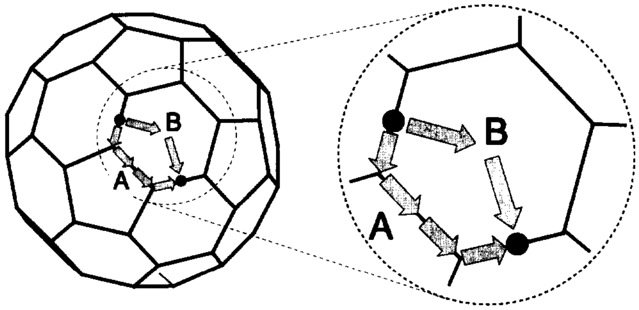

6 (η^6) of the six membered ring as shown in path **B** in the figure. Other paths between *A* and *B* or across the five-membered ring can also be envisioned. Whatever path is chosen, the total metal 4d and 5s overlap populations with the C_{60} in Table 2 show that the intermediate sites are net repulsive. The mechanism for movement of the metal to different positions on the surface of C_{60} is probably by dissociation and recombination. This is supported by experiment. It has been found in proceeding from the monosubstituted $(C_2H_5)_3Pt$ derivative of C_{60} to the hexasubstituted $(C_2H_5)_3Pt$ derivative, in which the platinums are oriented octahedrally on the C_{60}, that intermediate substitutions involve orientations that do not lead to the octahedral sites [3]. It was concluded from this work that the platinum fragments are able to attach to and dissociate from different sites on the C_{60} surface in proceeding to the sterically favored octahedral structure.

The factors which favor Pd bonding at the **2″** site are also apparent from examination of the resultant

TABLE 2. Mulliken orbital population analysis for palladium orbitals coordinated to various small ligands and C_{60} sites

	Methyl	Ethylene	Cp	Bz	C_{60} Site 1	C_{60} Site 2′	C_{60} Site 2″	C_{60} Site 5	C_{60} Site 6
Pd $4d_{xz}$ population	1.995	1.628	1.637	1.594	1.967	1.769	1.713	1.810	1.865
Pd 5s population	0.319	0.241	0.038	0.007	0.112	0.172	0.220	0.027	−0.030
Pd total 4d overlap population	+0.088	+0.096	+0.022	+0.086	−0.024	−0.004	+0.033	−0.117	−0.211
Pd $4d_{xz}$ overlap population	−0.021	+0.166	+0.010	−0.001	−0.036	+0.072	+0.105	−0.051	−0.107
Pd 5s overlap population	+0.189	+0.087	−0.132	−0.123	−0.009	−0.029	+0.016	−0.165	−0.242

molecular orbitals. The five highest occupied molecular orbitals of $C_{60}Pd$ correspond to the d^{10} configuration of the Pd atom. The most stable of these five orbitals is 63% Pd $4d_{xz}$ and 27% delocalized into the C_{60}. The C_{60} portion of this orbital is a mixture of the h_u and t_{1u} symmetry orbitals that results in the reasonably localized electron distribution shown in Fig. 4. The net interaction is bonding and is the single most important factor in stabilizing the coordination of the metal. The next three occupied orbitals are more than 97% Pd $4d_{x^2-y^2}$, $4d_{xy}$, and $4d_{xz}$ in character, and are primarily nonbonding. The HOMO of $C_{60}Pd$ (2″) is 82% Pd $4d_{z^2}$, 9% Pd 5s, and most of the rest from the C_{60} h_u symmetry orbitals. This orbital represents the donation from C_{60} to the metal 5s, but the presence of the metal $4d_{z^2}$ orbital sets up a filled–filled interaction that is net repulsive in this orbital. The lowest unoccupied orbitals are derived from the C_{60} t_{1u} orbitals. The first two are more than 99% t_{1u} in character. The next is 91% t_{1u}, 5% Pd $4d_{xz}$, and 3% Pd $5p_x$. This orbital is the antibonding counterpart of the filled d_{xz} to C_{60} bonding combination. The surface contour diagram in Fig. 4 shows that, unlike the bonding combination, this orbital remains delocalized across the C_{60} portion in these calculations.

Optimization of the geometries can have an influence on the magnitude of these results. Geometrical distortions of C_{60} are likely to be most important when the metal is bound at the **2″** position, because this is the position with the strongest interaction and electron delocalization. In order to examine the sensitivity of the results to geometrical distortions, we also performed calculations with the Pd atom bound to the **2″** site of a C_{60} that is distorted as found in crystal structures. For comparison, the bonding to a distorted ethylene ligand was also evaluated. The C–C bond distance of ethylene was taken from the crystal structure of $[(C_6H_5)_3P_2]Pt(\eta^2\text{-}C_2H_4)$ [31]. This distance is 1.434 Å, which is about 0.1 Å longer than the free ligand value. The hydrogens were bent back such that the CH_2 plane formed an angle of 27° with the CC vector as found from an *ab initio* molecular orbital calculation on $(PH_3)_2Pt(\eta^2\text{-}C_2H_4)$ [19,32]. For the distortion of C_{60}, two approaches were taken. First, the coordinates from the crystal structure of $[(C_6H_5)_3P_2]\text{-}Pt(\eta^2\text{-}C_{60})$ were used directly [5,33]. The C–C bond distance of the coordinated carbons is 1.502 Å, which is similar to that found in other structures and about 0.13 Å longer than the distance in free C_{60}. The metal-coordinated carbons are pulled out from the C_{60} sphere such that the angle of the plane formed by each coordinated carbon and the next carbon atoms in the C_{60} with the vector of the coordinated carbon atoms is about 40°. Unfortunately, the accuracy of the carbon atom positions from the crystals structures is only about 0.03 Å, and several other C–C distances are also 1.5 Å or greater in length. An additional calculation with an idealized distortion was also carried out so that the results would not be dependent on errors in the structure. The idealized distortion stretched the coordinated carbons to a distance of 1.5 Å from each other and from the next carbon atoms. This geometry is similar to that optimized by the *ab initio* calculations [19]. The results of these calculations were similar for these two representations of the distortion of C_{60}. It is found that the amount of donation from the metal to the ligand is sensitive to the distortion. The donation to the distorted ethylene increases to about 0.5 e^- compared with about 0.4 e^- for the undistorted ethylene, and the donation to the distorted C_{60} increases to about 0.4 e^- compared with about 0.3 e^- to the undistorted C_{60}.

In all of these cases, the bonding of the metal to C_{60} is weaker than to the corresponding small ligand. This situation does not improve in going from Ag^+ to Pd^0 except in the case of of the bonding to the **2″** position,

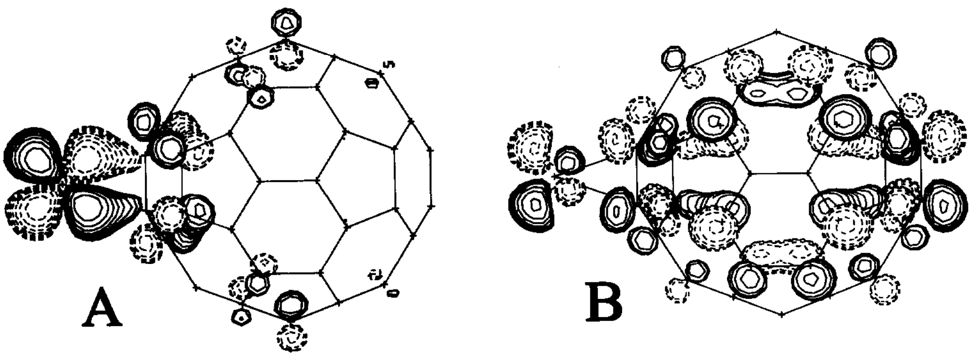

Fig. 4. Orbital surface plots (value = ±0.03) for the occupied orbital which shows the backbonding from the metal d_{xz} to the C_{60} (A), and for the virtual orbital which is the antibonding counterpart (B).

where the donation from the metal d_{xz} orbital to C_{60} becomes more competitive in comparison to ethylene. Specifically, for Ag^+ the donation of the d_{xz} to C_{60} is 55% of that to ethylene, for Pd^0 it is 77%. In our previous study, we also compared the bonding of C_{60} and ethylene to platinum in the complexes $(PH_3)_2Pt(\eta^2\text{-}C_{60})$ and $(PH_3)_2Pt(\eta^2\text{-}C_2H_4)$ [17]. This third row Pt atom with phosphine donor ligands is expected to be a much stronger donor group than a bare Pd atom, and in these calculations we found the bonding of C_{60} and ethylene to be virtually indistinguishable by this method. Apparently, as the donor ability of the metal improves, the bonding of C_{60} becomes more competitive with that of ethylene. After submitting the paper on our Fenske-Hall calculations of $(PH_3)_2Pt(\eta^2\text{-}C_{60})$ and $(PH_3)_2Pt(\eta^2\text{-}C_2H_4)$ in March of 1992, a comparison of these two Pt complexes by an *ab initio* molecular orbital method was reported in 1993 [19]. These calculations showed a net donation of 0.925 e^- to C_{60} in comparison to 0.347 e^- to ethylene. The much improved donor ability of the metal that occurs in these calculations results in a C_{60} that is coordinated more strongly than ethylene. This relative bonding is consistent with the metal complexes that have been prepared to this time. For example, the $[(C_6H_5)_3P_2]Pt(\eta^2\text{-}C_{60})$ complex is made by displacement of ethylene from $[(C_6H_5)_3P_2]Pt(\eta^2\text{-}C_2H_4)$ [5]. $Ir(CO)Cl(PPh_3)_2$ forms a stable complex with C_{60} [9], but is ineffective in the uptake of ethylene [34]. The relative amount of charge donated by the metal is evidenced by the CO stretching frequencies of these complexes. For $(\eta^5\text{-indenyl})Ir(CO)(C_{60})$ the CO stretching frequency is 1998 cm^{-1}, which is about 30 cm^{-1} greater than the stretching frequency of the corresponding ethylene complex [12]. This is a clear indication that C_{60} is removing more electron density from this metal center than ethylene. In a similar study of adducts of $Ir(CO)Cl(PPh_3)_2$, Balch finds that the C_{60} complex removes less electron density from the metal than electron deficient alkenes such as C_2F_4 and TCNE [9]. In terms of electron withdrawing ability, C_{60} seems to be most similar to O_2 [9] or dimethylfumarate [35].

An experimental estimate of the charge on the coordinated C_{60} cluster can be obtained from the redox potential [36]. The redox potential of $[(C_6H_5)_3P_2]Pt(\eta^2\text{-}C_{60})$ lies about halfway between the reduction of C_{60} and the reduction of C_{60}^-. It has been shown that this redox process is largely localized on the C_{60} [37]. Electrostatically, the C_{60} in $[(C_6H_5)_3P_2]Pt(\eta^2\text{-}C_{60})$ behaves like it has a charge of about -0.3 to -0.5 electrons. Our calculation on $(PH_3)_2Pt(\eta^2\text{-}C_{60})$ using the crystal structure coordinates gives a total charge on C_{60} of -0.34 electrons. Our previous calculation with an undistorted C_{60} gave a charge of about -0.5 electrons. Thus the theoretical results, although extremely approximate, give a reasonable representation of the experimental measurements.

To summarize this series of calculations, we see that the bonding of a metal to the surface of C_{60} is sensitive to the site of coordination, the geometrical distortions that can take place, and the electron richness of the metal. Coordination at the 2″ site is always most favored, as expected from the nature of the HOMO and the LUMO, although coordination at the 2′ site is nearly as effective. As the orbital contour plots show, numerous orbitals of C_{60} in the frontier region are utilized in the bonding. A metal which attempts to move across the surface of the C_{60} from one 2″ site to an adjacent 2′ site or another 2″ site must pass through conformations (such as η^1, η^5 or η^6) that are repulsive according to these calculations.

Acknowledgements

We thank P.J. Fagan and J.R. Shapley for helpful discussions. We also thank P.J. Fagan for providing the atomic coordinates of $(\eta^2\text{-}C_{60})Pt(PPh_3)_2$. D.L.L. acknowledges support by the US Department of Energy (Division of Chemical Sciences, Office of Basic Energy Sciences, Office of Energy Research, DF-SG02-86ER13501) for small molecule interactions with metals, the National Science Foundation (Grant No. CHE8519560) for contributions to the equipment and the support of L.L.W. as a visiting Research Faculty, and the Materials Characterization Program, Department of Chemistry, University of Arizona. N.E.G. acknowledges the financial support of the Department of Chemistry, University of Arizona in the form of a fellowship.

References and notes

1 (a) H.W. Kroto, J.R. Heath, S.C. O'Brien, R.F. Curl and R.E. Smalley, *Nature*, *318* (1985) 162; (b) R.F. Curl and R.E. Smalley, *Science*, *242* (1988) 1017; (c) W. Krätschmer, L.D. Lamb, K. Fostiropoulos and D.R. Huffman, *Nature*, *347* (1990) 354.
2 (a) D.R. Huffman, *Physics Today*, *44* (11) (1991) 22; (b) H.W. Kroto, A. Wallaf and S.P. Balm, *Chem. Rev.*, *91* (1991) 1213; (c) for an excellent review, see *Acc. Chem. Res.*, *25* (1992) 97; (d) R. Taylor and D.R.M. Walton, *Nature*, *363* (1993) 685.
3 P.J. Fagan, J.C. Calabrese and B. Malone, *Acc. Chem. Res.*, *25* (1992) 134 and references cited therein.
4 A.L. Balch, V.J. Catalano, W.L. Joong, M.M. Olmstead and S.R. Parkin, *J. Am. Chem. Soc.*, *113* (1991) 8953.
5 P.J. Fagan, J.C. Calabrese and B. Malone, *Science*, *252* (1991) 1160.
6 S.A. Lerke, B.A. Parkinson, D.H. Evans and P.J. Fagan, *J. Am. Chem. Soc.*, *114* (1992) 7807.
7 B. Chase and P.J. Fagan, *J. Am. Chem. Soc.*, *114* (1992) 2252.
8 P.J. Fagan, J.C. Calabrese and B. Malone, *J. Am. Chem. Soc.*, *113* (1991) 9408.
9 A.L. Balch, V.J. Catalano and J.W. Lee, *Inorg. Chem.*, *30* (1991) 3980.

10 A.L. Balch, J.W. Lee, B.C. Noll and M.M. Olmstead, *Inorg. Chem.*, *32* (1993) 3577.
11 A.L. Balch, V.J. Catalano, J.W. Lee and M.M. Olmstead, *J. Am. Chem. Soc.*, *114* (1992) 5455.
12 R.S. Koefod, M.F. Hudgens and J.R. Shapley, *J. Am Chem. Soc.*, *113* (1991) 8957.
13 J.A. Howard, M. Tomietto and D.A. Wilkinson, *J. Am. Chem. Soc.*, *113* (1991) 7870.
14 M. Rasinkangas, T.T. Pakkanen, T.A. Pakkanen, M. Ahlgren and J. Rouvinen, *J. Am. Chem. Soc.*, *115* (1993) 4901.
15 V.V. Bashilov, P.V. Petrovskii, V.I. Sokolov, S.V. Lindeman, I.A. Guzey and Y.T. Struchkov, *Organometallics*, *12* (1993) 991.
16 (a) D.S. Marynick and S. Estreicher, *Chem. Phys. Lett.*, *132* (1986) 383;
(b) P.D. Hale, *J. Am. Chem. Soc.*, *108* (1986) 6087;
(c) M.D. Newton and R.E. Stanton, *J. Am. Chem. Soc.*, *108* (1986) 2469;
(d) S. Larsson, A. Volosov and A. Rosén, *Chem. Phys. Lett.*, *137* (1987) 501;
(e) R.C. Haddon, L.E. Brus and K. Raghavachari, *Chem. Phys. Lett.*, *125* (1986) 459;
(f) S. Satpathy, *Chem. Phys. Lett.*, *130* (1986) 545;
(g) H.P. Lüthi and J. Almlöf, *Chem. Phys. Lett.*, *135* (1987) 357;
(h) J.W. Mintmire, B.I. Dunlap, D.W. Brenner, R.C. Mowrey and C.T. White, *Phys. Rev. B*, *43* (1991) 14281;
(i) E. Burstein, S.C. Erwin, M.Y. Jiang and R.P. Messmer, The charge state of C_{60} (Buckminsterfullerene) molecules adsorbed on a metal surface: theoretical considerations, *Physica Scripta*, in press;
(j) B.I. Dunlap, D.W. Brenner, J.W. Mintmire, R.C. Mowrey and C.T. White, Local density functional electronic structures of three stable icosahedral fullerenes, *J. Chem. Phys.*, *95* (1991) 8737.
17 D.L. Lichtenberger, L.L. Wright, N.E. Gruhn and M.E. Rempe, *Synthetic Metals*, *59*(3) (1993) 353.
18 J.R. Rogers and D.S. Marynick, *Chem. Phys. Lett.*, *205* (2,3) (1993) 197.
19 N. Koga and K. Morokuma, *Chem. Phys. Lett.*, *202*(3,4) (1993) 330.
20 (a) M.J.S. Dewar, *Bull. Soc. Chim. Fr.*, *18* (1951) C79; (b) J. Chatt and L.A. Duncanson, *J. Chem. Soc.*, (1953) 2939.
21 H. Nagashima, A. Nakaoka, Y. Saito, M. Kato, T. Kawanishi and K. Itoh, *J. Chem. Soc., Chem. Commun.*, (1992) 377.
22 M.B. Hall and R.F. Fenske, *Inorg. Chem.*, *11* (1972) 768.
23 MOPLOT2 is a program written by Dr. Dennis Lichtenberger to plot electron density results from Fenske-Hall calculations.
24 D.L. Lichtenberger and G.E. Kellogg, *Acc. Chem. Res.*, *20* (1987) 379.
25 G.E. Scuseria, *Chem. Phys. Lett.*, *176* (1991) 423.
26 S. Liu, Y-J. Lu, M.M. Kappes and J.A. Ibers, *Science*, *254* (1991) 408.
27 K. Hedberg, L. Hedberg, D.S. Bethune, C.A. Brown, H.C. Dorn, R.D. Johnson and M. De Vries, *Science*, *254* (1991) 410.
28 A. Rathna and J. Chandrasekhar, *Indian J. Chem, Sec. A&B*, *31* (1992) F51.
29 (a) T. Chen, S. Howells, M. Gallagher, L. Yi, D. Sarid, D.L. Lichtenberger, K.W. Nebesny and C.D. Ray, *Mat. Res. Soc. Symp. Proc*, *206* (1991) 721;
(b) T. Chen, S. Howells, M. Gallagher, L. Yi, D. Sarid, D.L. Lichtenberger, K.W. Nebesny and C.D. Ray, *J. Vac. Sci. Tech.*, *9*(5) (1991) 2461;
(c) D. Sarid, T. Chen, S. Howells, M. Gallagher, L. Yi, D.L. Lichtenberger, K.W. Nebesny and C.D. Ray, *Ultramicroscopy*, *42* (1992) 610.
30 E.A. Cartner and W.A. Goddard, III, *Surface Science*, *209* (1989) 243.
31 P.T. Cheng and S.C. Nyburg, *Can. J. Chem.*, *50* (1972) 912.
32 K. Morokuma and W.T. Borden, *J. Am. Chem. Soc.*, *113* (1991) 1912.
33 We thank Paul J. Fagan for supplying these coordinates.
34 L. Vaska, *Acc. Chem. Res.*, *1* (1968) 335.
35 J.R. Shapley, personal communication.
36 S.A. Lerke, B.A. Parkinson, D.H. Evans and P.J. Fagan, *J. Am. Chem. Soc.*, *114* (1992) 7807. P.J. Fagan, personal communication.
37 R.S. Koefod, C. Xu, W. Lu, J.R. Shapley, M.G. Hill and K.R. Mann, *J. Phys. Chem.*, *96* (1992) 2928.